IChemE

0263–8762/96/$07.00 + 0.00

THE LAMINAR AND TURBULENT FLOW PATTERN OF A PITCHED BLADE TURBINE

A. BAKKER[1], K. J. MYERS[2], R. W. WARD[2] and C. K. LEE[3]

[1]*Chemineer, Inc, Dayton, Ohio, USA*
[2]*University of Dayton, Dayton, Ohio, USA*
[3]*The Dow Chemical Company, Midland, Michigan, USA*

The flow field generated by the pitched-blade turbine in both laminar and turbulent operation has been investigated using laser Doppler velocimetry (LDV) and digital particle image velocimetry (DPIV) experimental techniques. This data has been used to critically evaluate the performance of computational fluid mixing (CFM) tools. It has been found that current CFM software can accurately predict the laminar flow behaviour of the pitched-blade impeller if the proper velocity boundary conditions are provided around the entire periphery of the impeller. In turbulent operation, CFM simulations predict some of the features of the flow field, but dramatically underpredict the total energy dissipation rate in the vessel. They are not currently capable of describing the large-scale instabilities in the flow detected by DPIV.

Keywords: mixing; stirred tank; pitched blade turbine; laser-Doppler; particle image velocimetry; turbulence

INTRODUCTION

As the use of computational simulation becomes more widespread for the analysis and design of mixing processes, see Bakker *et al.*[1] and Bakker and Van den Akker[2], it is important to critically examine the capabilities of these tools. This is necessary for the development of guidelines for the proper application of current simulation software, to place limits on the expected accuracy of this software, and to direct the development of the next generation of simulation software.

Because of its industrial importance, the laminar and turbulent operation of the pitched-blade impeller has been chosen for this evaluation of computational fluid mixing (CFM) simulation. The experimental tools used in this study are the conventional laser Doppler velocimetry (LDV) and the novel digital particle image velocimetry (DPIV). The combination of these experimental tools provides accurate point values of time-averaged and fluctuating velocities, as well as the time-averaged and semi-instantaneous flow fields in an agitated vessel.

EXPERIMENTS

Figure 1 shows the sketch of the tank that was used in the LDV measurements. The tank is 0.145 m in diameter. The liquid level is equal to the tank diameter. The impeller is a pitched blade impeller with a blade width of $W/D = 0.188$ and a 45° blade angle. The impeller to tank diameter ratio was $D/T = 0.35$. The impeller to bottom clearance was $C/T = 0.46$. The baffle width was 0.0127 m and the baffle had zero clearance to the wall. Silicone oil, a Newtonian fluid, was used in the laminar flow experiments. It has a viscosity of $\mu = 0.211$ Pa s and a density of $\rho = 1049\,\text{kgm}^{-3}$. The experiments were conducted at 100 rpm, resulting in an impeller Reynolds number of $Re = 21$. The impeller Reynolds number is defined as:

$$Re = \frac{\rho N D^2}{\mu} \tag{1}$$

In the turbulent experiments the liquid was water. These experiments were conducted at 500 rpm. The Reynolds number is 21 500.

The LDV system utilizes a dual channel, 2 watt argon ion laser. A PC controlled transversing mechanism is used to move the laser probe in a pre-determined grid. An Aerometrics Doppler signal analyser and data

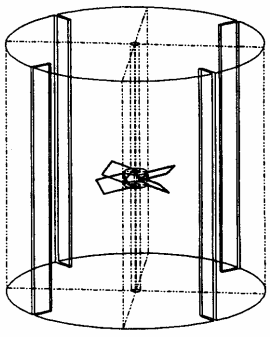

Figure 1. Outline of the tank used in the LDV experiments and the CFM simulations.

acquisition and processing software was used. In this work, only one channel of the LDV was used at a time to get a single velocity component. The other two velocity components were obtained by readjusting the laser beams, so that all three velocity components obtained would correspond to the same location within the tank. Velocity data were taken at a vertical (axial-radial) plane along a baffle. An almost uniformly spaced (5 mm × 5 mm) grid was set up to map out the velocity distribution at this plane. In the region around the boundary of the impeller, data were collected in a denser grid (2 mm spacing), since these data were used as CFD simulation inputs. The seed particles were metallic coated spherical particles. The density of the seed particles was 2600 kgm^{-3} with an average diameter of 12 μm. In a typical velocity measurement using back-scattering mode, a criterion of 3600 validated points or six minute time period was set as the end of data acquisition for the laminar case. Most of the averaged data had around 3000 validated points in the laminar flow regime, while up to 30 000 validated points were taken in the turbulent flow regime. Selected data points were measured again to check for reproducibility. Results showed that the averaged velocities were reproducible within 5%. However, when the velocities were very close to zero, variations were much greater due to insufficient validated points.

Additional experiments were performed using a Dantec Flowgrabber™, digital particle image velocimetry system. In these experiments the flow field was seeded with small flow-flowing fluorescent particles. The particle diameter was 8×10^{-5} m. The tank is illuminated with a sheet of laser light, 10 mm thick, generated by an Argon-Ion laser. The motion of the particles in the light sheet is filmed with a CCD camera. The images of the CCD camera are digitized and the flow field is extracted from these images by cross-correlating successive images. More details of the measurement technique can be found in Willert and Gharib[3], Myers *et al.*[4] and Ward[5]. The tank used in the DPIV experiments was 0.292 m in diameter and was kept as closely geometrically similar to the tank used in the LDV experiments as possible. Small differences were that the impeller blade width was slightly larger—$W/D = 0.2$—and that there was a small spacing between the baffles and the wall. The baffle width was $T/12$ and the baffle to wall spacing was $T/72$. The Reynolds number in the DPIV experiments was $Re = 10\,000$.

Laser Doppler velocimetry is a point measurement technique. Accurate velocity measurements can be performed one point at a time. Time averaged flow fields can then be constructed by performing successive measurements at various points in the flow domain. In contrast, DPIV is a semi-instantaneous full flow field measurement technique. The whole flow field is measured at once, during the time it takes the camera to record two images, here $2 \times 0.033 = 0.066$ seconds. DPIV is therefore more suited for studying time varying flow fields than LDV, provided that the resolution of the camera is high enough to accurately record the smallest structures of interest. However, LDV is more suited for accurately recording time series of local velocities. The information generated by both these flow measurement techniques should therefore be regarded as complementary.

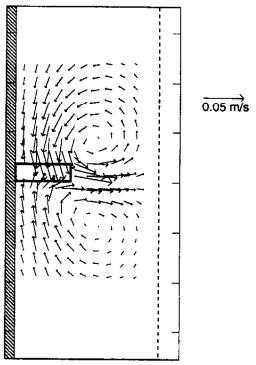

Figure 2. Velocity vector plot of the LDV results for the laminar flow pattern in the 0.145 m tank. $Re = 21$.

EXPERIMENTAL RESULTS

Figure 2 shows velocity vector plots of the experimental data for the laminar case. The flow pattern was measured in the baffle plane. The impeller generates a mainly radial flow pattern, with very low velocities away from the impeller. Two small circulation loops form, one above and one below the impeller plane. In effect the impeller creates a 'cavern' of fast moving liquid close to the impeller, with very little movement farther from the impeller.

Figure 3 shows the time averaged flow pattern as measured with both the LDV system and the DPIV system for the turbulent cases. Since the experiments were performed on two different scales and impeller speeds, the data were normalized with the impeller tip

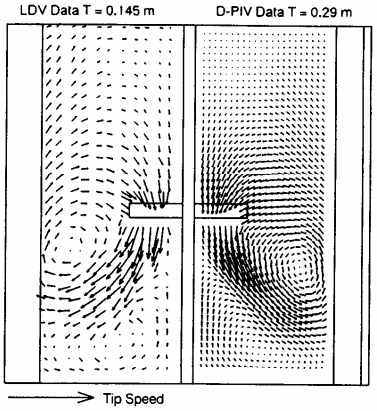

Figure 3. Comparison between the time averaged turbulent flow pattern as measured with LDV and as measured using DPIV.

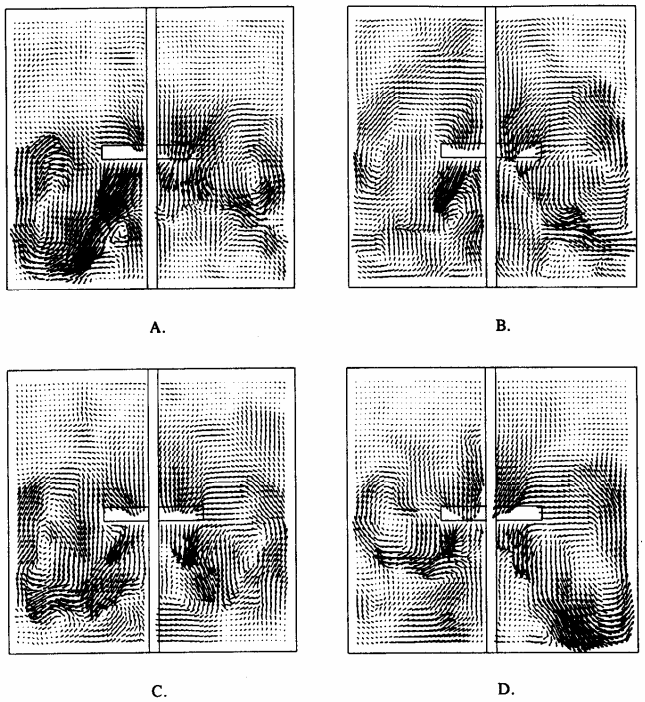

Figure 4. Four semi-instantaneous flow pattern measurements, using the DPIV system under turbulent flow conditions in the 0.292 m tank. $Re = 10\,000$.

speed and tank diameter. The impeller discharge appears like that associated with an axial flow pattern. However, due to the relatively large impeller to bottom clearance, a second flow loop is created in the bottom part of the tank. The agreement between the LDV and the DPIV results is reasonable. The size of the bottom circulation loop is a little bit larger in the LDV experiment, but that may be caused by the difference in baffling. While the baffles were attached to the wall in the LDV experiment, there was a small clearance between the baffles and the wall in the DPIV experiment.

The results shown in Figure 3 are time averaged. Bakker and Van den Akker[2] found bimodal velocity distributions in certain regions in a similar stirred tank and suggested that this type of flow exhibits periodic oscillations. The DPIV system employed here allows semi-instantaneous flow field measurements. The DPIV results in Figure 3 are an average of 1024 measurements over a period of about 20 minutes. Figure 4 shows some semi-instantaneous flow fields. It can be seen that none of these semi-instantaneous flow fields is the same as the time average, shown in Figure 3. At any point the flow may be severely asymmetrical and very chaotic. Further investigation revealed the presence of large scale flow pattern instabilities with a time scale much longer than the impeller rotational frequency[5]. The flow pattern is highly unsteady. However, when a sufficient number of these chaotic semi-instantaneous flow fields are averaged, the final result is the smooth flow pattern shown in Figure 3. These results show that both the LDV and the DPIV system give similar results for the time averaged flow patterns, but that the time averaged flow patterns may be somewhat misleading when compared to the chaotic flow in the tank. These large scale chaotic flow structures may well be responsible for much of the efficient mixing in turbulent stirred tanks.

LAMINAR FLOW SIMULATIONS

The flow pattern simulations were performed with the general purpose fluid flow simulation program Fluent™ V4.2. The simulations were performed for the 0.145 m diameter tank shown in Figure 1. For the laminar flow simulations, the velocities measured with the LDV system were prescribed around the entire impeller periphery. It was found that it was necessary to prescribe the rotational velocity of the shaft to obtain correct predictions of the tangential velocities in the top of the tank. The simulations were performed using three-dimensional grids with 41 000 grid cells for a 90° section of the tank.

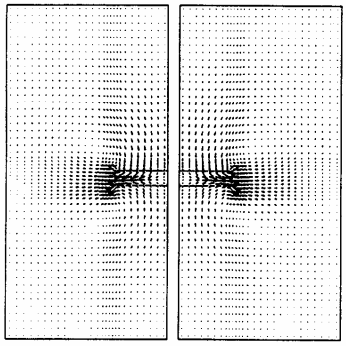

Figure 5. Velocity vector plot of the results of the simulation of the laminar flow pattern in the 0.145 m tank using the LDV data as impeller boundary conditions. Plane between the baffles. $Re = 21$.

The results of the laminar flow pattern simulations are shown in Figures 5 to 7. Figure 5 shows a velocity vector plot. Figure 6 shows the velocity magnitude in the tank. Large velocities are found in the immediate vicinity of the impeller. Away from the impeller the velocities are very low. The impeller generates a predominantly radial flow pattern. Figure 7 shows the magnitude of the tangential velocity in the tank. Comparison of Figures 6 and 7 shows that the overall velocity magnitude is only slightly higher than the tangential velocity. This means that the flow in the tank is dominated by the tangential velocity, rather than by axial or radial pumping action.

Figure 8 shows a quantitative comparison between the measured and predicted axial, radial and tangential velocities respectively. The axial velocities are predicted

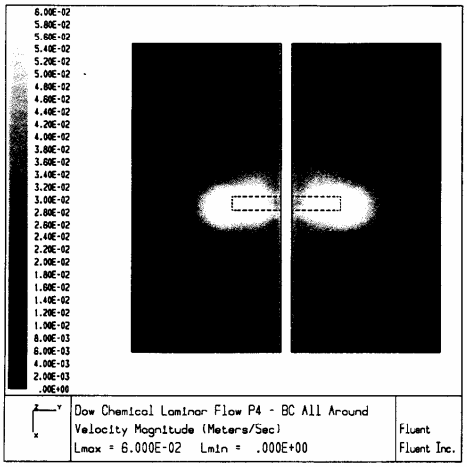

Figure 6. Gray scale raster of the velocity magnitude for the simulations of Figure 5.

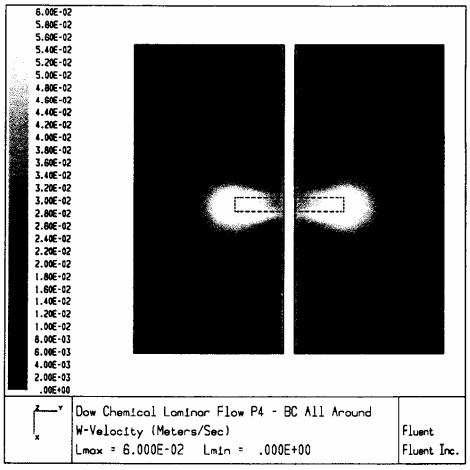

Figure 7. Gray scale raster of the tangential velocity for the simulations of Figures 5 and 6.

extremely well. The predictions of the radial and tangential velocities are slightly less accurate, but in general the accuracy of the model predictions is more than satisfactory.

TURBULENT FLOW PATTERN SIMULATIONS

The velocities measured with the LDV system at the bottom outflow of the impeller were prescribed as impeller boundary conditions, as were the turbulent kinetic energy density k and the energy dissipation rate density ϵ. The values for ϵ were calculated from k assuming that in the outflow of the impeller the Taylor macro-scale of turbulence was equal to one-fourth of the impeller blade width, see Bakker and Van den Akker[2]. The simulations were performed using three-dimensional grids with 39 000 grid cells for a 90° section

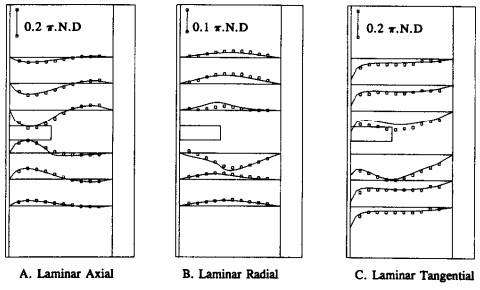

Figure 8. Comparison between the experimental LDV data and the results of the CFM simulations for the laminar flow pattern. $Re = 21$. In (A) values above the baselines are upwards directed axial velocities. In (B) velocities above the baselines are inward directed radial velocities. In (C) values below the baselines are tangential velocities in the direction of the impeller rotation.

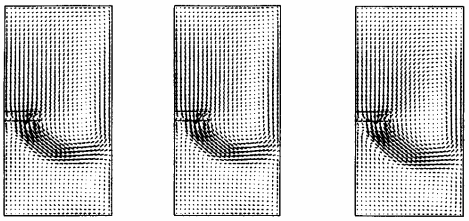

Figure 9. Velocity vector plots of the results of the CFM simulations for the turbulent flow pattern using three different turbulence models. $Re = 21\,500$.

of the tank. In the CFM model the flow pattern was assumed to be steady. Three different turbulence models were tested, the k-ϵ model, the k-ϵ RNG model and the Reynolds stress model (RSM). The k-ϵ RNG model is a modification of the standard k-ϵ model that is reported to perform better for flows with strong curvature or separations[6].

Figure 9 shows the flow pattern predictions in a plane between the baffles, using the k-ϵ, k-ϵ RNG and RSM turbulence models respectively. When comparing these

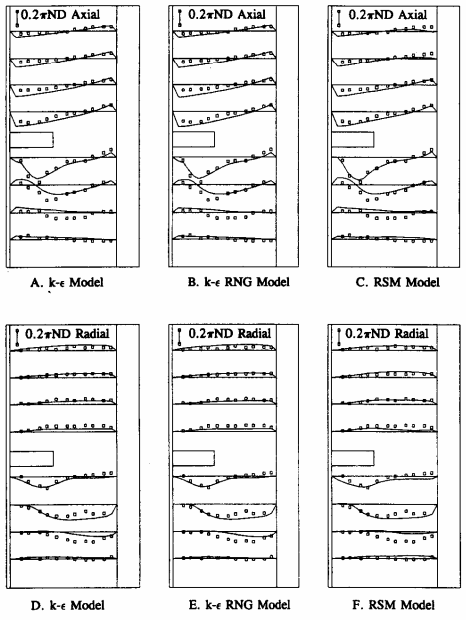

Figure 10. Comparison between the experimental LDV data and the results of the CFM simulations for the turbulent flow pattern. In (A) to (C) values above the baselines are upwards directed axial velocities. In (D) to (F) velocities above the baselines are inward directed radial velocities. $Re = 21\,500$. The results with three different turbulence models are being compared.

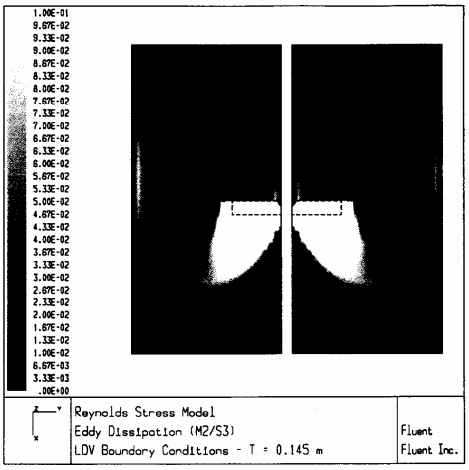

Figure 11. The local dissipation rate ϵ as predicted using the RSM turbulence model, in a plane midway between the baffles. $Re = 21\,500$.

results with the experimental results in Figure 3, it can be seen that the flow pattern is qualitatively correct but that the secondary circulation loop at the tank bottom is too large, with all three turbulence models. Figure 10 shows a direct comparison between the predictions and the experimental data for the axial and the radial velocities respectively. In general the predictions follow the trends in the experimental data quite well, although the accuracy is not as good as would be desired.

Figures 9 and 10 show that there is very little difference between the predictions using the three turbulence models. The k-ϵ and the k-ϵ RNG model basically predict the same flow pattern. The predictions of the RSM model are slightly different only in the top part of the tank, near the baffle (compare the top lines in Figure 10(b) and 10(c)) and in the bottom circulation loop (compare the two bottom lines in Figures 10(e) and 10(f)).

Figure 11 shows the turbulent energy dissipation rate ϵ in a plane midway between the baffles as predicted using the RSM turbulence model. The spatial distribution of ϵ is highly non-uniform with extremely high values close to the impeller and low values in the liquid bulk. To evaluate the accuracy of the predictions for the turbulence levels in the tank the turbulent energy dissipation rate ϵ was integrated over the whole vessel to obtain the overall energy dissipation rate, which should equal the impeller power draw. From the overall value of ϵ an impeller power number was calculated. Several other turbulence quantities were calculated also. The turbulent viscosity μ_t is defined as:

$$\mu_t = C_\mu \frac{k^2}{\epsilon} \tag{2}$$

Here C_μ is a model constant with a value of 0.09 as used in the turbulence modelling. The Taylor macro scale of

Table 1. Various overall turbulence parameters calculated from the Fluent predictions.

Model Used	*Po*	$\langle\mu_t\rangle/\mu$	$\langle L_t\rangle/T$	$\langle L_k\rangle/T$	$\langle k\rangle$
k-ϵ	0.64	95.2	0.12	7.5E–4	3.8E–3
k-ϵ-RNG	0.63	91.4	0.12	7.6E–4	3.7E–3
RSM	0.72	51.7	0.08	7.8E–4	2.7E–3

turbulence L_T was calculated as:

$$L_T = \frac{k^{3/2}}{\epsilon} \tag{3}$$

The Kolmogorov micro scale of turbulence is defined as:

$$L_k = \left(\frac{\nu^3}{\epsilon}\right)^{1/4} \tag{4}$$

Here ν is the kinematic viscosity of the fluid. The turbulent kinetic energy density k is defined as:

$$k = \frac{1}{2}\sum_{i=1}^{3}\overline{u_i u_i} \tag{5}$$

Here u_i is the fluctuation component of the liquid velocity in direction i. The vessel averaged values are denoted with parentheses, e.g. the vessel averaged value of k is denoted as $\langle k\rangle$. The turbulent viscosity, made dimensionless with the molecular viscosity, is a measure of the amount of momentum transport due to turbulent eddies relative to the momentum transport due to the molecular viscosity. The Taylor macro scale is a measure of the largest turbulent eddies in the vessel. The Kolmogorov micro scale is a measure of the smallest eddies in the vessel. Both turbulent length scales are made dimensionless with the tank diameter T. The results are listed in Table 1. The averaged values were for μ_t, L_t and L_k were calculated by integrating the local values of these quantities over the volume of the tank. Due to the non-uniform distributions of these variables, this results in different values for the averages than if they were calculated from the vessel average values of ϵ and k directly.

The experimentally measured power number, *Po*, was 1.2 for this impeller. The impeller power number is implicitly defined by:

$$P = Po\rho N^3 D^5 \tag{6}$$

Here P is the power draw of the impeller. The power number predicted by the CFM model is between 40% and 48% too low depending on the turbulence model used. The RSM turbulence model gives the best prediction with a power number of 0.72. There are two effects that lead to the underprediction of the power number. First, all energy dissipated through shear at the impeller blades or through trailing vortices behind the impeller blades is not accounted for in this simplified impeller model. Second, it is assumed that the flow is steady. As mentioned before, this type of flow will exhibit large scale instable flow structures. Energy dissipated through these large scale instabilities is therefore unaccounted for. To obtain correct predictions of both the overall flow field and the energy dissipation it may be necessary to perform time dependent calculations using a sliding mesh model for the impeller[7,8].

The predictions for the ratio between the turbulent viscosity and the molecular viscosity varies between 51.7 and 95.2, depending on the turbulence model used. This means that turbulent eddies transport between 51.7 and 95.2 more momentum than the molecular velocity. The molecular viscosity therefore has little effect at high values of Reynolds number.

The predictions for the Taylor macro scale vary between 0.08 and 0.12 times the tank diameter. This means that the largest eddies found in this tank will have a size of 0.08 to 0.12 times the tank diameter. The predictions for the smallest eddy size, the Kolmogorov length scale, vary between 7.5×10^{-4} and 7.8×10^{-4} times the tank diameter. The RSM turbulence model predicts a lower value of the overall turbulent kinetic energy density (2.7×10^{-3}) than the k-ϵ type turbulence models (3.7×10^{-3} to 3.8×10^{-3}). This causes the turbulent viscosity μ_t to be lower and allows the RSM to handle flows with more curvature or swirl.

CONCLUSIONS

In laminar operation, LDV data indicates that the pitched-blade turbine pumps radially rather than axially, flow is confined to the region near the impeller, and tangential motion dominates the flow. Given the proper boundary conditions (velocities) around the entire periphery of the impeller, current CFM software can predict this behaviour both qualitatively (the radial flow pattern) and quantitatively (the actual velocity magnitudes). However, it is important to include the influence of the rotating shaft to ensure proper predictions of the tangential velocity.

In turbulent operation, the time-averaged flow fields measured by DPIV and LDV show reasonable agreement. However, DPIV clearly indicates that the time-averaged flow pattern of the pitched-blade turbine has little relation to the semi-instantaneous flow behaviour in the vessel. On a time-averaged basis the pitched-blade turbine pumps axially. However, because of the high impeller off-bottom clearance studied, the discharge flow impinges on the vessel wall and the flow at the base of the vessel is directed radially inward. Given the proper impeller discharge velocities, CFM predicted this flow pattern with all three turbulence models studied. However, the region of reversed flow predicted by CFM was substantially larger than that found experimentally for the time averaged flow patterns. As the DPIV results show that the flow is highly unsteady, these results suggest that the steady state models used here are not adequate for describing the flow in such reactors.

The laminar flow simulations showed that the method of prescribing experimentally measured impeller boundary conditions results in accurate flow pattern predictions. The fact that when the same technique is used to model a turbulent stirred tank significant discrepancies between the experimental data and the simulations are found, must be due to the turbulence model, and/or the flow instabilities of the system which are not captured in a steady state model.

CFM predictions of the total energy dissipation rate in turbulent operation varied between the three turbulence models. These differences between models was much

smaller than the difference between model predictions and experimental measurements, however. It is possible that the significant portion of input energy not accounted for in the turbulent simulations is contained in the large-scale instabilities of the flow as detected by DPIV. These large-scale fluctuations in the turbulent flow field may be responsible for much of the mixing. It is suggested to direct future research efforts towards the study of these unsteady flow patterns. CFM models that describe the time dependent flow in the full tank need to be developed, possibly using sliding mesh methodology.

NOMENCLATURE

C	impeller to bottom clearance, m
D	impeller diameter, m
k	turbulent kinetic energy density, $m^2 s^{-2}$
$\langle k \rangle$	vessel averaged value of k, $m^2 s^{-2}$
L_k	Kolmogorov micro scale of turbulence, m
$\langle L_k \rangle$	vessel averaged value of L_k, m
L_t	Taylor macro scale of turbulence, m
$\langle L_t \rangle$	vessel averaged value of L_t, m
Po	impeller power number
Re	Reynolds number
T	vessel diameter, m
ν	kinematic viscosity, $m^2 s^{-1}$
W	blade width, m

Greek letters

ϵ	turbulent energy dissipation rate density, $m^2 s^{-3}$
μ	dynamic viscosity, Pa s
μ_t	turbulent viscosity, Pa s
$\langle \mu_t \rangle$	vessel averaged value of μ_t, Pa s
ρ	density, kgm^{-3}

REFERENCES

1. Bakker, A., Fasano, J. B. and Leng, D. E., 1994, Pinpoint mixing problems with lasers and simulation software, *Chem Eng*, January: 94–100.
2. Bakker, A. and Van den Akker, H. E. A., 1994, Single-phase flow in stirred reactors, *TransIChemE*, 72(A4): 583–593.
3. Willert, C. E. and Gharib, M., 1991, Digital particle image velocimetry, *Experiments in Fluids, Volume 10*, 181–193.
4. Myers, K. J., Ward, R. W., Bakker, A. and Fasano, J. B., 1995, A DPIV investigation of flow pattern instabilities of axial-flow impellers, *Mixing XV, 15th Biennial North American Mixing Conference, June 18–23, 1995, Banff, Canada.*
5. Ward, R. W., 1995, A DPIV investigation of flow pattern instabilities of axial-flow impellers, *MSc Thesis* (School of Engineering, University of Dayton).
6. Fluent, 1995, *Fluent User's Guide Version 4.3*, volume 4, chapter 19.
7. Murthy, J. Y., Mathur, S. R. and Choudhury, D., 1994, CFD simulations of the flows in stirred tank reactors using a sliding mesh technique, *8th European Conference on Mixing, IChemE Symposium Series No 136* (IChemE), 341–348.
8. Bakker, A., LaRoche, R. D., Calabrese, R. V. and Wang, M. H., 1995, Sliding mesh simulations of the flow pattern of axial pumping impellers at low and intermediate Reynolds numbers, *Mixing XV, 15th Biennial North American Mixing Conference, June 18–23, Banff, Canada.*

ACKNOWLEDGEMENT

The authors wish to acknowledge the help of James W. Nordmeyer in performing the DPIV experiments.

ADDRESS

Correspondence concerning this paper should be addressed to Dr A. Bakker, Chemineer Inc, 5870 Poe Avenue, Dayton, Ohio 45414-1123, USA.